Effect of Short Regions of Surface Curvature on Compressible Turbulent Boundary Layers*

David Degani†
Technion—Israel Institute of Technology, Haifa, Israel
and
Alexander J. Smits‡
Princeton University, Princeton, New Jersey

Calculations were performed to investigate the supersonic flow of a turbulent boundary layer over short regions of concave surface curvature. The freestream Mach number was 2.9 upstream of each curved surface. Three different constant radii of curvature wind-tunnel models were investigated to cover a range of curvature and turning angles. The numerical technique solved the full, Reynolds-averaged Navier-Stokes equations using two different turbulence models: an algebraic eddy-viscosity model, and a one-equation model. The calculations were compared with recent experimental data, and the agreement with the mean-flow results was surprisingly good, especially for the computations using the one-equation model. The computed Reynolds shear stress results tended to fall below the experimental values as the radius of curvature decreased, demonstrating the shortcomings of the turbulence models for rapidly perturbed flows. Some limiting cases for zero radius of curvature (compression corner flows) were also investigated, and the results appear to show a periodic unsteadiness similar to that observed in recent experiments.

Nomenclature

C_f = skin-friction coefficient
$\bar{E},\bar{F}$ = inviscid flux vectors in Cartesian coordinates
$\hat{E},\hat{F}$ = inviscid flux vectors in general coordinates
f = frequency, Hz
J = transformation Jacobian
L = characteristic length
P = pressure
P_∞ = freestream pressure
$\bar{q}$ = dependent-variables vector in Cartesian coordinates
$\hat{q}$ = dependent-variables vector in general coordinates
R = longitudinal radius of curvature
$\bar{R},\bar{S}$ = viscous flux vectors in Cartesian coordinates
$\hat{R},\hat{S}$ = viscous flux vectors in general coordinates
R_e = Reynolds number
S = Strouhal number, $f\delta_o/U_\infty$
t = time
U = velocity component in x direction
U_τ = friction velocity
U_∞ = freestream velocity
x,y = physical Cartesian coordinate axes
α = corner angle
Δt = nondimensional timestep
δ_o = boundary-layer thickness
η,ξ = commutational coordinate axes
ν = kinematic viscosity
τ = computational time

Introduction

IN this investigation, we calculate the behavior of a supersonic turbulent boundary layer experiencing a short region of concave surface curvature. Within the curved region, the boundary layer experiences the combined effects of an adverse pressure gradient, bulk compression, and concave streamline curvature.

Longitudinal curvature, bulk compression, longitudinal pressure gradient, (and streamline divergence), are examples of what Bradshaw[1] called "extra" strain rates, that is, strain rates additional to the main shear $\partial U/\partial y$. Experience has shown that even relatively small extra strain rates can have very significant effects on the flow behavior. For instance, a small amount of concave curvature in a zero pressure-gradient subsonic flow amplifies the turbulence levels strongly, increases the turbulence length scales, and produces longitudinal roll cells through a Taylor-Goertler-like instability.[2-4] In a supersonic flow, similar effects appear to occur. For example, Thomann[5] obtained heat-transfer data for a zero pressure gradient, Mach 2.5 turbulent boundary layer on a concavely curved wall, and found that even weak curvature dramatically increased the heat-transfer rates.

Little is known, however, regarding the simultaneous action of different extra strain rates. They appear to interact strongly, and the interaction can be extremely complex. For example, Smits et al.[6] found that a boundary layer experiencing the simultaneous effects of concave curvature and streamline divergence did not exhibit the turbulence amplification expected if each effect were added linearly. Nor did the boundary layer show any evidence for the presence of longitudinal roll cells (see also Smits and Joubert[7] and Smits and Wood[8]). These studies indicated that the amplification of longitudinal vorticity by concave curvature and the amplification of spanwise vorticity by divergence possibly interact nonlinearly to prevent the formation of steady longitudinal vortices.

In the present case of a compressible flow over a concavely curved wall, curvature acts in combination with bulk compression and longitudinal pressure gradient. Similar flow geometries were investigated by McLafferty and Barber,[9] Hoydysh and Zakkay,[10] Chou and Childs,[11] and especially Sturek and Danberg[12,13] and Laderman.[14] The results, however, gave

*Due to an error in our editorial office, an incorrect version of this paper was published in the January 1989 issue of this journal. The version presented here is the revised and correct one.

Presented as Paper 85-1667 at the AIAA 18th Fluid Dynamics, Plasmadynamics and Lasers Conference, Cincinnati, OH, July 16-18, 1985; received Nov. 19, 1986; revision received April 27, 1988.

†Associate Professor, Faculty of Mechanical Engineering. Member AIAA.

‡Associate Professor, Department of Mechanical and Aerospace Engineering. Member AIAA.

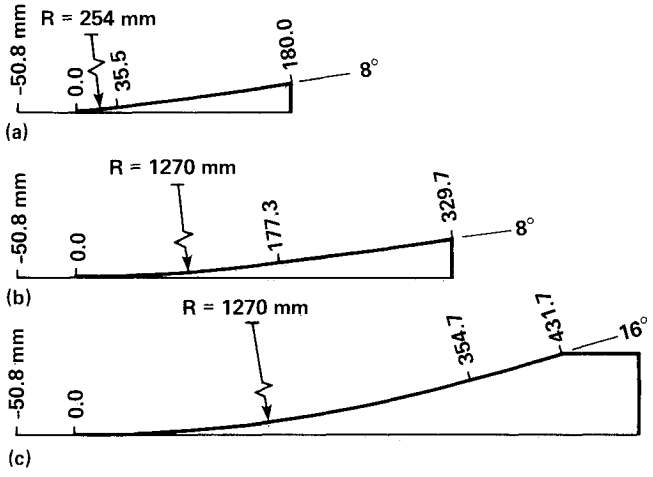

Fig. 1 Test model geometries: a) model 1; b) model 2; and c) model 3.

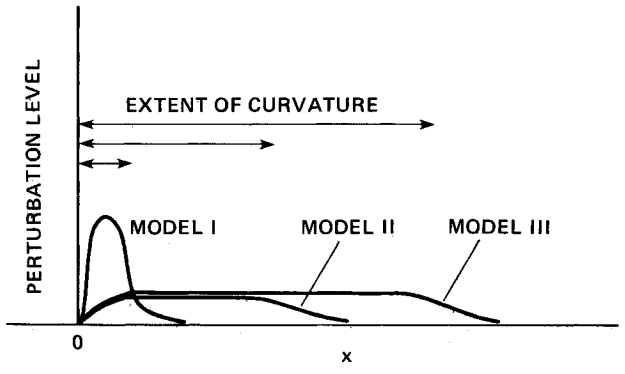

Fig. 2 Qualitative distributions of longitudinal pressure gradient, along a streamline originating at $y/\delta_o = 0.5$.

little indication regarding the relative influence of each effect, and they provided little insight into the influence of perturbation rate; that is, the effect of changing the distance over which the curvature or pressure rise is applied.

Previous calculations of compressible flows with streamline curvature and pressure gradient are limited in number. The early work by Bradshaw[15] was restricted to plane walls with adverse pressure gradients, and later work has usually focused on the computation of shock-wave/boundary-layer interactions.[16,17] The Sturek and Danberg flow, however, has been calculated by several workers, and the results were summarized by Rubesin et al.[18] The turbulence models used in these calculations ranged from a single mixing-length relationship to a full Reynolds-stress model, and the reults were rather contradictory. For example, the mixing-length model predicted the mean velocity profiles fairly well but the agreement with the skin-friction distribution was poor. Yet, the Reynolds-stress model gave precisely the opposite results. When taken as a whole, these calculations demonstrate how difficult it is to predict complex, compressible flows.

To improve our understanding of curved, compressible boundary-layer flows, Taylor and Smits[19] and Jayaram et al.[20] recently tested the three wind-tunnel models shown in Fig. 1. For model 1, the ratio of initial boundary-layer thickness to radius of curvature δ_o/R was 0.1, and the turning angle was fixed at 8 deg; for model 2, δ_o/R was 0.02, and the turning angle was 8 deg; and for model 3, δ_o/R was 0.02, and the turning angle was 16 deg. Further experimental details may be found in Taylor.[21]

These three experiments tested the response of the boundary layer to a wide range of stress gradients or strain rates. This range is illustrated in Fig. 2, where the magnitudes of the pressure gradients are qualitatively shown. The area under each curve represents the overall pressure rise for each model. By examining a range of perturbation rates and strengths, the experiments serve as an excellent test case for turbulence models.

Two different turbulence models were used in the current calculations: the algebraic eddy-viscosity model due to Baldwin and Lomax[22] and the one-equation model due to Rubesin.[23] The Baldwin-Lomax model was chosen because of its widespread use in compressible-flow calculations, particularly where the boundary conditions are changing rapidly (see, for example, Visbal and Knight[24]). The version of the Rubesin model used here is due to Coakley et al.,[17] and it introduces an elementary history effect into the calculations. Although several turbulence models exist which include curvature corrections, none of them perform satsifactorily for concave walls or for cases with a small radius of curvature (especially when the radius of curvature tends to zero, as for the case of a sharp corner).[1,15,25] Furthermore, the combined effects of bulk compression and streamline curvature are not well understood,[7,26] and it is not clear how turbulence models may be modified to describe the interaction between such extra strain rates. Here, such curvature corrections were specifically excluded in order to determine the performance of the basic turbulence models in flows with widely varying streamline curvature and pressure gradient. Recent unpublished computations by Fernando and Donovan at Princeton, using the boundary-layer code developed by Bradshaw,[27] indicate that the empirical corrections required to take account of compressibility and curvature effects were significant in that case. In the present study, the turbulence models were used in numerical solutions of the full, Reynolds-averaged Navier-Stokes equations using an implicit approximate factorization finite-difference algorithm, and one of the aims of these calculations is to determine the need for empirical extra strain-rate correction in this context.

II. Governing Equations

The strong conservation law form of the Navier-Stokes equations in general coordinates can be written in nondimensional form as

$$\frac{\partial \hat{q}}{\partial \tau} + \frac{\partial \hat{E}}{\partial \xi} + \frac{\partial \hat{F}}{\partial \eta} = Re^{-1}\left[\frac{\partial}{\partial \xi}(\hat{R}^{\xi} + \hat{R}^{\eta}) + \frac{\partial}{\partial \eta}(\hat{S}^{\xi} + \hat{S}^{\eta})\right] \quad (1)$$

The inviscid flux vectors in Eq. (1) are

$$\hat{q} = \bar{q}/J \quad (2a)$$

$$\hat{E} = (\xi_t \bar{q} + \xi_x \bar{E} + \xi_y \bar{F})/J \quad (2b)$$

$$\hat{F} = (\eta_t \bar{q} + \eta_x \bar{E} + \eta_y \bar{F})/J \quad (2c)$$

and the viscous flux vectors are

$$\hat{R} = \hat{R}^{\xi}(\bar{q}, \bar{q}_{\xi}) + \hat{R}^{\eta}(\bar{q}, \bar{q}_{\eta}) = (\xi_x \bar{R} + \xi_y \bar{S})/J \quad (3a)$$

$$\hat{S} = \hat{S}^{\xi}(\bar{q}, \bar{q}_{\xi}) + \hat{S}^{\eta}(\bar{q}, \bar{q}_{\eta}) = (\eta_x \bar{R} + \eta_y \bar{S})/J \quad (3b)$$

An implicit approximate factorization finite-difference algorithm is used to solve Eq. (1). Further details of the numerical technique and the treatment of the boundary and initial conditions may be found in Refs. 28 and 29. Briefly, a 120×48 grid was used for all calculations, and the resolution near the wall was maintained such that the mesh size normal to the wall was less than $5\nu/u_\tau$. The grid spacing in the streamwise direction was fine in the curvature region ($\Delta x/\delta_o = 0.045$) and stretched to a coarser grid [$(\Delta x/\delta_o)_{\max} = 0.64$] upstream and downstream of the curvature region.

Sutherlands's law is used to calculate the laminar viscosity. The effects of turbulence are simulated in terms of an eddy-

viscosity coefficient, using two different models: a zero- and a one-equation turbulence model.

For the zero-equation model, the Baldwin-Lomax algebraic model[22] is used without any modification for the curvature. The one-equation model (or kinetic energy equation model) uses an additional partial differential equation to calculate the eddy-viscosity coefficients. The model that is used in the present work (without any modification for the curvature) was formulated by Rubesin[23] for compressible flows, based on the Glushko[30] model for incompressible flat plate boundary-layer flows. Coakley et al.[17] used a simpler version of Rubesin's model where certain compressibility terms, which involve first derivatives of the temperature, were omitted (these terms were found to have a negligible effect by Viegas and Coakley[16]).

III. Results

To obtain the initial profile for the computations, the flow on a flat plate was calculated and adjusted until the upstream Reynolds number based on boundary-layer thickness matched the value observed in the experiment. For both the computations and the experiment, the stagnation pressure was 6.9×10^5 N/m^2 (100 psia), and the incoming flow had a freestream Mach number of 2.87 with a unit Reynolds number

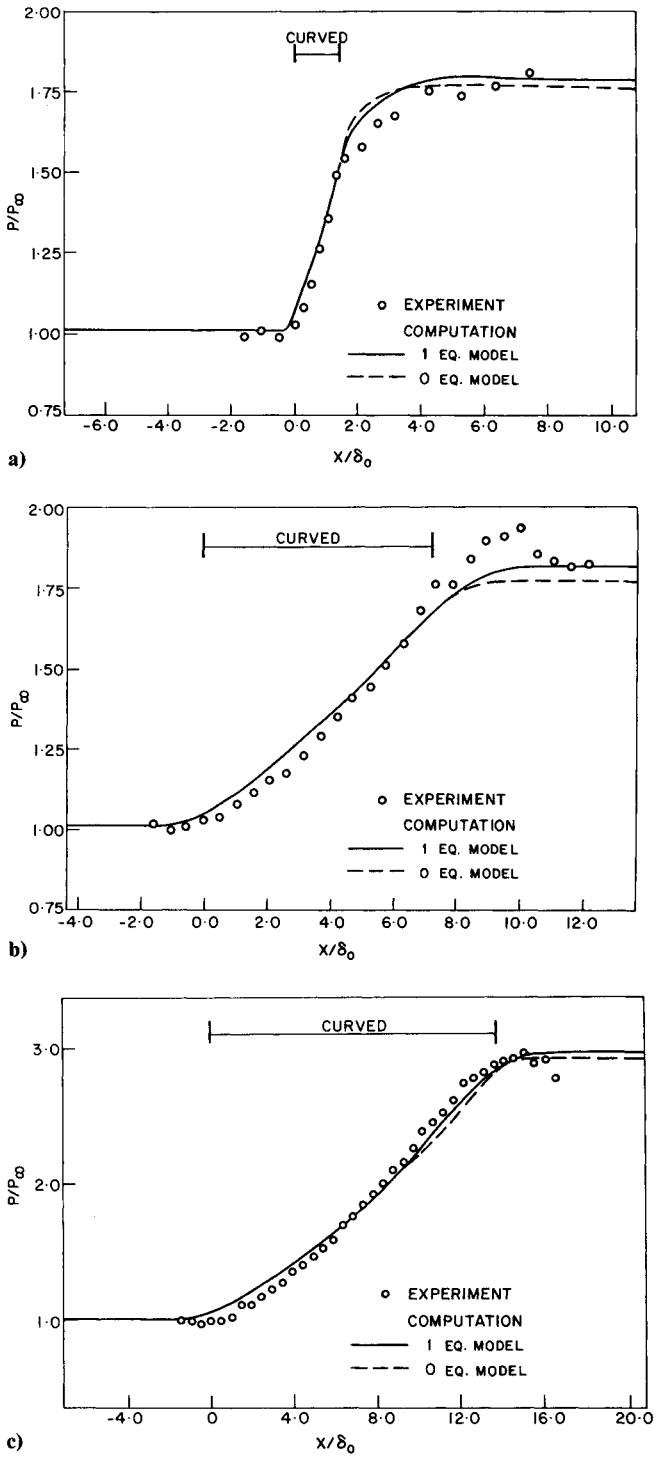

Fig. 3 Comparison between calculated and experimental pressure distributions: a) model 1; b) model 2; and c) model 3.

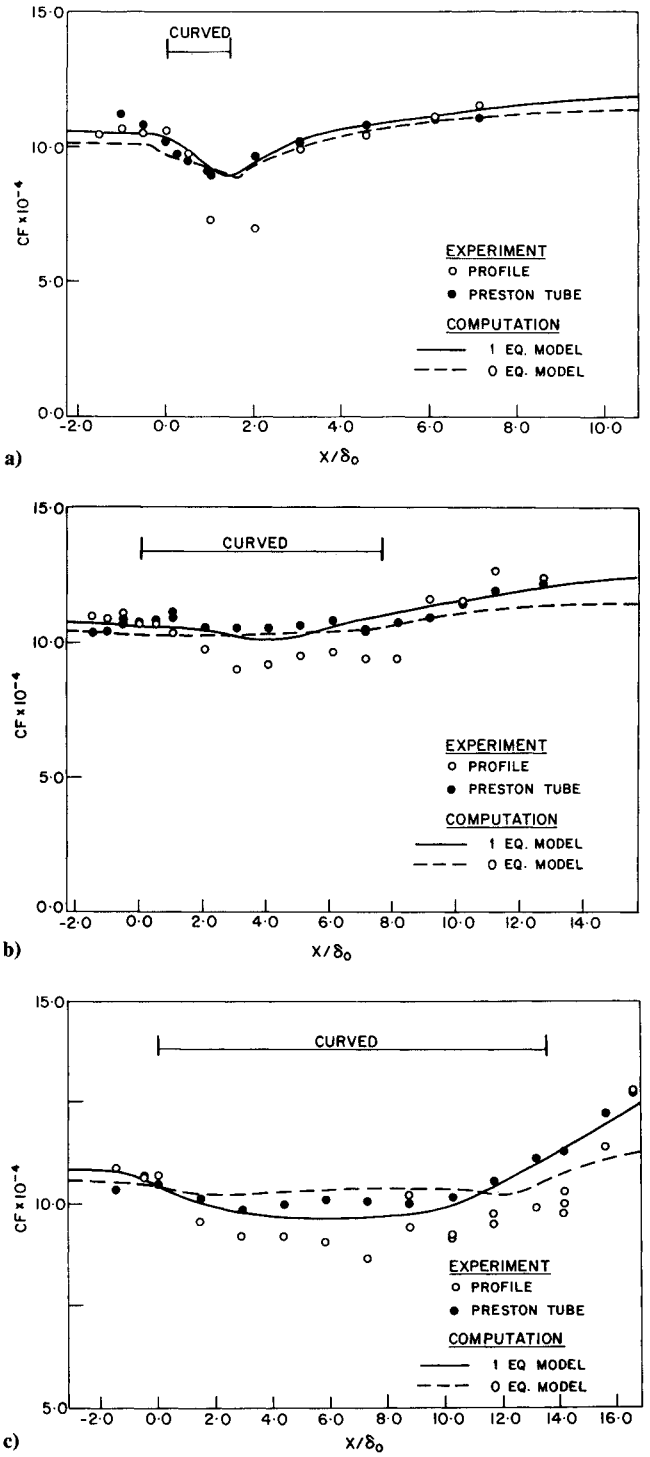

Fig. 4 Comparison between calculated and experimental skin-friction coefficient distributions: a) model 1; b) model 2; and c) model 3.

of 6.3×10^7/m. The wall conditions were assumed to be adiabatic. The incoming turbulent boundary layer developed in a zero pressure gradient, and just upstream of each model the boundary-layer thickness δ_o was 26 mm.

The x coordinate was defined as the streamwise direction, and it was measured along the surface of the model with the origin at the beginning of curvature. The y coordinate was measured normal to the wall.

The calculated wall static pressures are compared with the experimental values in Fig. 3. The results show good qualitative agreement, but quantitatively the agreement is not so satisfactory. For example, the calculation does not reproduce the rather slow pressure rise observed in the model 1 experiment downstream of the curvature, and the pressure gradients for model 3 are underestimated. Note that the slight overshoot in the pressure for model 2 is probably due to a spurious wave system originating from the tunnel ceiling. The two turbulence models give almost identical results in the curved region, but in every case the one-equation model predicts a slightly higher downstream level. The differences, however, are not significant, and the two calculations bracket the value corresponding to the wedge at the final turning angle.

The skin-friction distributions are shown in Fig. 4. The results for both turbulence models demonstrate good agreement with experiment in the curved regions of all three flows, especially when we note that the experimental uncertainty in the absolute value of C_f in these regions is about $\pm 10\%$, and that the Preston tube values are probably more reliable than those deduced from the velocity profiles. (The principle difficulty in deducing C_f values in strongly perturbed supersonic flows seems to lie in defining the correct boundary-layer edge conditions. In the present case, this uncertainty significantly affects the accuracy of the values derived from the velocity profiles in the region of rapid pressure rise.[31]) Downstream in the recovery zone, however, the one-equation model clearly performs better than the algebraic model. The superiority of the one-equation model becomes more obvious as the perturbation strength and duration increases, and this trend demonstrates the importance of including flow-history effects in the calculation.

The calculated and experimental velocity profiles, shown in Fig. 5, agree closely in the outer part of the layer; that is, for $y/\delta > 0.2$. The differences between the two turbulence models are not really significant because the maximum experimental uncertainty is about $\pm 5\%$, whereas the calculations agree with the data to within 3 or 4%. Near the wall, the computations do not reproduce the "kinks" observed in the experimental profiles. When plotted in log-law coordinates, these kinks show up as "dips" below the log law, suggesting an increase in the rate of growth of the turbulence length scale with distance from the wall.[4,6] Both turbulence models have a fixed length-scale distribution, however, without any modification for curvature and cannot be expected to reproduce these dips below the log law.

The effects of curvature and compression are seen most clearly in the Reynolds shear stress profiles. In Fig. 6, the calculated values are compared with the experimental results for models 1 and 2 (one-equation turbulence model only). For model 2 ($\delta_o/R = 0.02$) the agreement is remarkable, but for model 1 ($\delta_o/R = 0.1$) the levels are consistently underpredicted. The discrepancies are not spectacular, but they indicate the growing importance of the curvature and compression effects as the distance over which the perturbation was applied decreases.

Finally, some interesting effects were observed while studying the limiting case where $R = 0$ (compression corner flow). The calculations for $\alpha = 20$ deg have already been presented by Degani and Steger.[28] This flow is separated, and a small separation bubble occurred near the corner. Degani and Steger reported that a small perturbation introduced into the calculated flowfield caused the separation bubble to oscillate at almost constant amplitude and frequency (about 1400 Hz). At

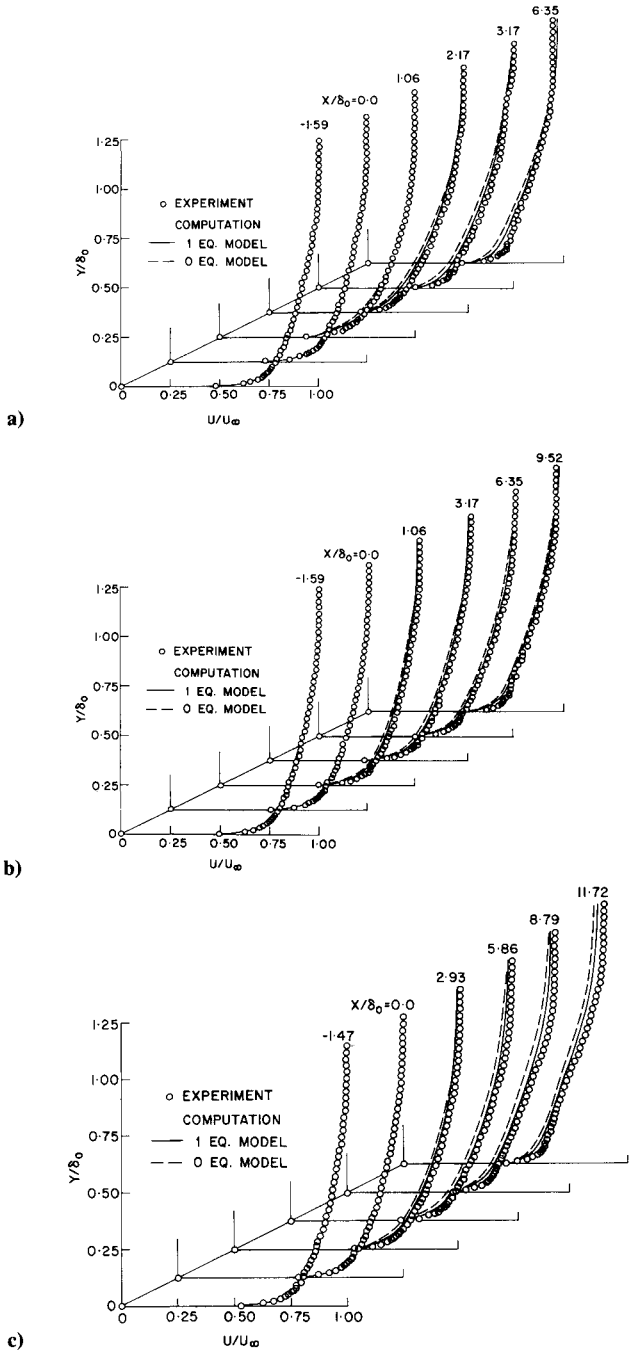

Fig. 5 Comparison between calculated and experimental velocity profiles: a) model 1; b) model 2; and c) model 3.

the time, it was thought to be due to a numerical interaction between the turbulence model and a flowfield. A similar unsteadiness was observed by Visbal[32] for $\alpha = 16$ deg. Visbal attributed the oscillation to variations in the very low values of the computed inner eddy viscosity, caused by the Van Driest damping factor approaching zero in the reattachment region.

What makes these observation so intriguing is that experimental investigations of the compression corner flows have shown an unsteadiness at about 1–2 kHz, although the frequency distribution of the flow unsteadiness was rather broad and strongly skewed.[34,37] To study this oscillation more closely, the case calculated by Degani and Steger was recomputed here for several different time steps and grid spacings. The results are summarized in Fig. 7 for the algebraic model. It was found that in order to converge to a constant frequency

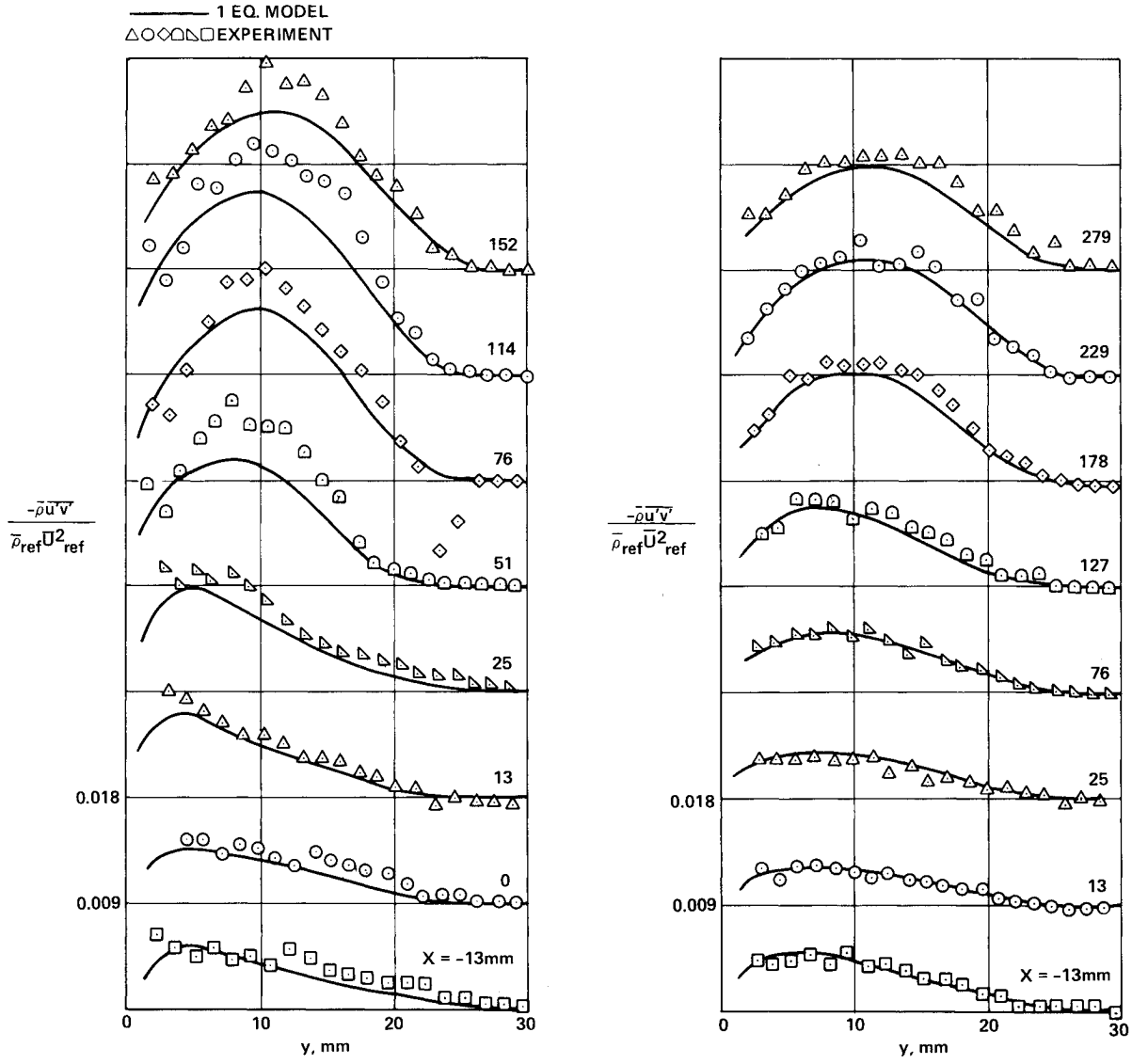

Fig. 6 Comparison of calculated shear stress with experimental values.[20]

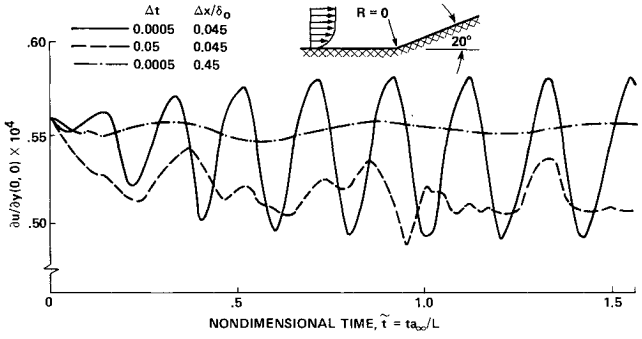

Fig. 7 Effect of nondimensional time step and grid size on unsteadiness.

oscillation, the nondimensional time step Δt must be small relative to the cycle time. Decreasing Δt below the value of 0.0005 resulted in a small change only. However, a coarser grid ($\Delta x/\delta_o = 0.45$) in the region of the bubble damped out the oscillation even for small Δt. These oscillations were limited to the region of the separation bubble. Similar results were obtained for the one-equation model (with up to 10% differences in frequency and amplitude).

It is suggested here that in the present calculations these oscillations were not introduced by the turbulence models. Careful study showed that the eddy-viscosity coefficients varied smoothly in the region of the bubble, and there was no indication of numerical instability that might cause oscillation. The oscillation damped out when the numerical smoothing was increased drastically, or when the eddy-viscosity coefficients were frozen to a fixed value (an action that has the same effect as increasing the smoothing coefficients in the computations).

This behavior was observed also for the 16-deg sharp corner but not for the 8-deg sharp corner where there was no separation and the velocity profiles do not have an inflection point.

To study the unsteadiness effect of the perturbation in cases where the corner had finite curvature, several cases of different radii were studied. It was found that for cases where the radius of the curvature R/δ_o was larger than 4, the initial perturbation died away and the flowfields did not show any oscillations. Figure 8 summarizes the results for the 20- and 16-deg cases (the case of 20 deg, $R = 0$ is taken from Ref. 28). It seems that when the curved wall eliminates the inflection in the velocity profiles, the results do not show any oscillation.

The dimensional frequency obtained in the calculations for the perturbed flowfield (≈ 1400 Hz) is in the range of frequencies observed experimentally. The calculated frequency is also an order of magnitude lower than the frequency of the energy containing eddies in the incoming boundary layer (for our case $U_\infty/\delta_o \approx 25{,}000$ Hz). In principle, the numerical approxima-

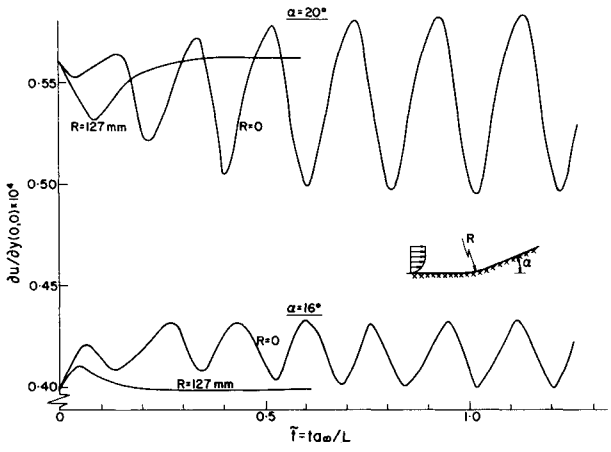

Fig. 8 Oscillations in the calculated velocity gradient as a function of the nondimensional time.

tion to the Navier-Stokes equations is capable of resolving such frequencies, and the results obtained in this paper are not an artifact of the numerical algorithm.

The frequencies observed in the two compression corner cases (16 deg. and 20 deg.) are about the same because the only characteristic length is the boundary-layer thickness upstream of the bubble (which is about the same for both cases), and the corresponding Strouhal number $S = f\delta_0/U_\infty$ is approximately constant.

IV. Discussion and Conclusions

The results demonstrate that a one-equation model is superior to an algebraic eddy-viscosity model for the calculation of short lengths of concavely curved, compressible flows. This conclusion holds over a range of perturbation intensities and duration, although for some quantities, such as the mean velocity, the differences between the models are not significant. Relative to the calculations of the Sturek and Danberg flow reported by Rubesin et al.[18] the performance of the algebraic model in the current computations was generally better than the performance of the algebraic eddy-viscosity model, while the one-equation results presented here were considerably better than any of the calculations summarized by Rubesin et al.[18] The effects of the curvature and compression extra strain rates appear to have a relatively minor influence, at least for the cases studied here. The most notable influence is seen in the predicted Reynolds shear stress levels which tend to underestimate the experimental values as the levels of the extra strain rate increases. The relative success of these Reynolds-averaged Navier-Stokes calculations strongly suggest that the need for empirical modifications to the turbulence length-scale distribution commonly used to account for curvature and compressibility effects[28] is partly driven by the use of the boundary-layer approximation.

Acknowledgment

NASA Ames Research Center provided financial support for the first author and the computational facilities for the calculations. The second author received support from NASA Langley Research Center under Grant NAG-1-545 (monitored by Mr. D. Haynes and Dr. W. Sawyer) during the course of this work.

References

[1]Bradshaw, P. "Effects of Streamline Curvature on Turbulent Flows," AGARDograph No. 169, Aug. 1973.

[2]So, R. M. and Mellor, G. L., "An Experimental Investigation of Turbulent Boundary Layers Along Curved Surfaces," NASA CR-1940, April 1972.

[3]Ramaprian, B. R. and Shivaprasiad, B. G., "The Structure of Turbulent Boundary Layers Along Mildly Curved Surfaces," *Journal of Fluid Mechanics*, Vol. 85, 1978, pp. 273-303.

[4]Smits, A. J., Young, S. T. B., and Bradshaw, P., "The Effect of Short Regions of High Surface Curvature on Turbulent Boundary Layers," *Journal of Fluid Mechanics*, Vol. 94, 1979, pp. 209-242.

[5]Thomann, H., "Effect of Streamwise Curvature on Heat Transfer in a Turbulent Boundary Layer," *Journal of Fluid Mechanics*, Vol. 33, Pt. 2, 1968, pp. 283-292.

[6]Smits, A. J., Eaton, J. A., and Bradshaw, P., "The Response of Turbulent Boundary Layer to Lateral Divergence," *Journal of Fluid Mechanics*, Vol. 94, 1979, pp. 243-268.

[7]Smits, A. J. and Joubert, P. N., "Turbulent Boundary Layers on Bodies of Revolution," *Journal of Ship Research*, Vol. 26, 1982, pp. 135-147.

[8]Smits, A. J. and Wood, D. H., "The Response of Turbulent Boundary Layers to Sudden Perturbations," *Annual Review of Fluid Mechanics*, Vol. 17, 1985, pp. 321-358.

[9]McLafferty, G. H. and Barber, R. E., "The Effect of Adverse Pressure Gradient on the Characteristics of Turbulent Boundary Layers in Supersonic Streams," *Journal of the Aerospace Sciences*, Vol. 29, Jan. 1969, pp. 1-10.

[10]Hoydysh, W. G. and Zakkay, V., "An Experimental Investigations of Hypersonic Turbulent Boundary Layers in Adverse Pressure Gradient," *AIAA Journal*, Vol. 7, Jan. 1969, pp. 105-116.

[11]Chou, J. H. and Childs, M. E., "An Experimental Study of Surface Curvature Effects on a Supersonic Turbulent Boundary Layer," AIAA Paper 83-1672, 1983.

[12]Sturek, W. B. and Danberg, J. E., "Supersonic Turbulent Boundary Layer in an Adverse Pressure Gradient. Part I: The Experiment," *AIAA Journal*, Vol. 10, 1972, pp. 475-480.

[13]Sturek, W. B. and Danberg, J. E., "Supersonic Turbulent Boundary Layer in an Adverse Pressure Gradient. Part II: Data Analyis," *AIAA Journal*, Vol. 10, 1972, pp. 630-636.

[14]Laderman, A. J., "Adverse Pressure Gradient Effects on Supersonic Boundary-Layer Turbulence," *AIAA Journal*, Vol. 18, Oct. 1980, pp. 1186-1195.

[15]Bradshaw, P., "The Effect of Mean Compression or Dilatation on the Turbulence Structure of Supersonic Boundary Layers," *Journal of Fluid Mechanics*, Vol. 63, 1974, pp. 449-464.

[16]Viegas, J. R. and Coakley, T. J., "Numerical Investigation of Turbulence Models for Shock Separated Boundary-Layer Flows," AIAA Paper 77-44, Jan. 1977.

[17]Coakley, T. J., Viegas, J. R., and Horstman, C. C., "Evaluation of Turbulence Models for Three Primary Types of Shock Separated Boundary Layers," AIAA Paper 77-692, June 1977.

[18]Rubesin, M. W., Crisalli, A. J., Horstman, C. C., and Acharya, M., "A Critique of Some Recent Second-Order Closure Models for Compressible Boundary Layers," AIAA Paper 77-128, Jan. 1977.

[19]Taylor, M. and Smits, A. J., "The Effects of a Short Region of Concave Curvature on a Supersonic Turbulent Boundary Layer," AIAA Paper 84-0169, 1984.

[20]Jayaram, M., Taylor, M. W., and Smits, A. J., "The Response of a Compressible Turbulent Boundary Layer to Short Regions of Concave Surface Curvature," *Journal of Fluid Mechanics*, Vol. 175, 1987, pp. 343-362.

[21]Taylor, M. W., "A Supersonic Turbulent Boundary Layer on Concavely Curved Surfaces," Princeton Univ., Princeton, NJ, MAE Rept. 1684, Sept. 1984.

[22]Baldwin, B. S. and Lomax, H., "Thin-Layer Approximation and Algebraic Model for Separated Turbulent Flow," AIAA Paper 78-257, 1978.

[23]Rubesin, M. W., "One-Equation Model of Turbulence for Use with the Compressible Navier-Stokes Equations," NASA TM X-73-128, April 1976.

[24]Visbal, M. R. and Knight, D. D., "Evaluation of the Baldwin-Lomax Turbulence Model for Two-Dimensional Shock Wave Boundary-Layer Interactions," AIAA Paper 83-1697, 1983.

[25]Bradshaw, P., "Turbulent Flows with Extra Strain Rates," Zaric Memorial International Seminar on Wall Turbulence, Dubrovnik, Yugoslavia, May 1988. To be published Springer-Verlag.

[26]Jayaram, M. and Smits, A. J., "The Distortion of a Supersonic Turbulent Boundary Layer by Bulk Compression and Streamline Curvature," AIAA Paper 85-0299, 1985.

[27]Bradshaw, P. and Unsworth, K., "An Improved FORTRAN Program for Bradshaw-Feriss-Atwell Method of Calculating Turbulent Shear Layers," Aero-Report 74-02, Imperial College, University of London, London, UK, 1974.

[28]Degani, D. and Steger, J. L., "Comparison Between Navier-Stokes and Thin-Layer Computations for Separated Supersonic Flow," *AIAA Journal*, Vol. 21, 1983, pp. 1604–1606.

[29]Degani, D., "Numerical Algorithm Conjugating Steady and Transient, Separated, Compressible Flow and a Solid Body Having Arbitrarily Distributed Heat Sources," *Numerical Heat Transfer*, Vol. 7, 1984, pp. 395–411.

[30]Glushko, G. S., "Turbulent Boundary Layer on a Flat Plate in an Incompressible Fluid," *Bull. Acad. Sci. USSR*, Mech. Ser., No. 4, 1965, pp. 13–23.

[31]Fernando, E. M., Donovan, J. F., Smith, D. R., Smits, A. J., "Conventional Skin Friction Measurement Techniques for Strongly Perturbed Supersonic Turbulent Boundary Layers," AIAA Paper 89-1861, 20th Fluid and Plasma Dynamics and Lasers Conference, Buffalo, NY, June 1989.

[32]Visbal, M. R., "Numerical Simulation of Shock-Turbulent Boundary Layer Interactions over 2-D Compression Corners," Ph.D. Thesis, Rutgers University, 1983.

[33]Dolling, D. S. and Murphy, M., "Wall Pressure Fluctuations in a Supersonic Separated Compression Ramp Flowfield," AIAA Paper 82-0986, 1982.

[34]Andreopoulos, J. and Muck, K. C., "Some New Aspects of the Shock Wave Boundary Layer Interaction in Compression Ramp Flows," AIAA Paper 86-0342, 1986.